Characteristics of SMBI Fueling with Laval Nozzle in GAMMA 10 Based on Experimental and Simulation Results

M. M. Islam[1,a)], Y. Nakashima[1], S. Kobayashi[2], N. Nishino[3], K. Hosoi[1], K. Ichimura[1], M. S. Islam[1], K. Fukui[1], K. Shimizu[1], M. Ohuchi[1], M. Arai[1], T. Yokodo[1], G. Lee[1], M. Yoshikawa[1], J. Kohagura[1], M. Hirata[1], R. Ikezoe[1], M. Ichimura[1], M. Sakamoto[1] and T. Imai[1]

[1]*Plasma research center, University of Tsukuba, Tsukuba, Ibaraki 305-8577, Japan*
[2]*Institute of Advanced Energy, Kyoto University, Gokasyo, Uji 611-0011, Japan*
[3]*Graduate school of Engineering, Hiroshima University, Hiroshima 739-8527, Japan*

[a)]Corresponding author: maidul@prc.tsukuba.ac.jp

Abstract. Results of supersonic molecular bean injection (SMBI) with Laval nozzle has been carried out in the GAMMA 10 tandem mirror. The neutral transport during SMBI was investigated by the two-dimensional image of the light emission captured by the high-speed camera. We used the value of full width at half maximum (FWHM) of the distribution of emission intensity as an index of neutral transport. The FWHM value decreases with the increase of the plenum pressure which indicates that the particle diffusion was more convergent at high plenum pressure. Fully three-dimensional neutral transport simulation using a Monte-Carlo code DEGAS is applied to SMBI experiment and simulation results qualitatively explained the experimental results.

INTRODUCTION

In magnetically confined plasmas, optimization of particle fueling is a critical issue to obtain high performance plasmas. The supersonic molecular beam injection (SMBI) method developed by L. Yao et al. [1] is an effective fueling method for deeper penetration of neutral particles into the core plasma and high fueling efficiency compared to conventional gas-puff [2, 3]. SMBI system is very simple and economical to develop. An SMBI system has been applied to the GAMMA 10 device as a new particle fueling method to produce high density plasmas. A large tandem mirror device GAMMA 10 is an open magnetic plasma-confining device [4]. The SMBI system has been installed at the bottom of the central-cell at mid-plane. The central-cell is the main plasma confinement region in GAMMA 10 and have many observation port for analyzing the plasma behavior. Thus, the SMBI experiment is carried out at the central-cell. An SMBI experiment in GAMMA 10 has been performed by three conditions; without any nozzle, straight nozzle and Laval nozzle. The first experimental results of SMBI by both straight nozzle and without any nozzle showed that SMBI achieved higher density plasmas at the core region than the conventional gas puffing [5, 6]. In addition, the penetration depth is high in the case of straight nozzle than without nozzle [6]. Laval nozzle has been newly mounted at the SMBI valve in order to improve the effectiveness of fueling by SMBI. We investigate the neutral particles behavior during SMBI by using the Laval nozzle. The neutral transport is investigated based on the 2-D image captured by the high-speed camera. In the GAMMA 10 tandem mirror, the neutral transport code DEGAS [7] has been applied and simulation studied has been performed, investigating the neutral particle behavior in the tandem mirror device [8, 9]. Based on the experimental measurement, the detailed neutral distribution is predicted by using Monte-Carlo simulation.

EXPERIMENTAL SETUP

GAMMA 10 is the world largest tandem mirror plasma confining device, which consists of the central-cell, anchor-cells, plug/barrier cells and end cells. Figure 1(a) shows the schematic view of the GAMMA 10 tandem mirror, together with the diagnostics tools used in this study. GAMMA 10 is an effectively axisymmetrized minimum-B anchored tandem mirror with thermal barrier at both end-mirrors [10]. Initial plasma is produced by two plasma guns from both ends and then the main plasma is heated with two ion cyclotron radio frequency (ICRF) waves excited in the central-cell and anchor-cell, respectively. Two gas puffers are also installed for sustaining plasma at both mirror throat regions. The SMBI system consists of fast solenoid valve with a magnetic shield and a Laval nozzle.The total length of the Laval nozzle is 363 mm and the diameter of throat and exit sections are 0.6 mm and 24 mm, respectively. Figure 1(b) shows the cross-section view of the GAMMA 10 central-cell and outline of optical systems for the high-speed camera and the sketch of SMBI system. A high-speed camera has been installed at central-cell in order to observe the plasma behavior near the central limiter during SMBI. The high-speed camera observes the 2-dimensional (x-z, or y-z) response of plasma during SMBI and is suitably capable of measuring the light emission with a band of wavelength in visible light. The camera system has two lines of sight in the horizontal and vertical directions of the plasma cross-section by using dual blanch optical fiber bundles. The development of the injected molecular beam by SMBI in the axial (z) direction and the penetration depth into the plasma can be estimated from the 2-D image in two directions. The plenum pressure is 0.3 to 2.0 MPa and pulse width is usually 0.5ms during the experiment.

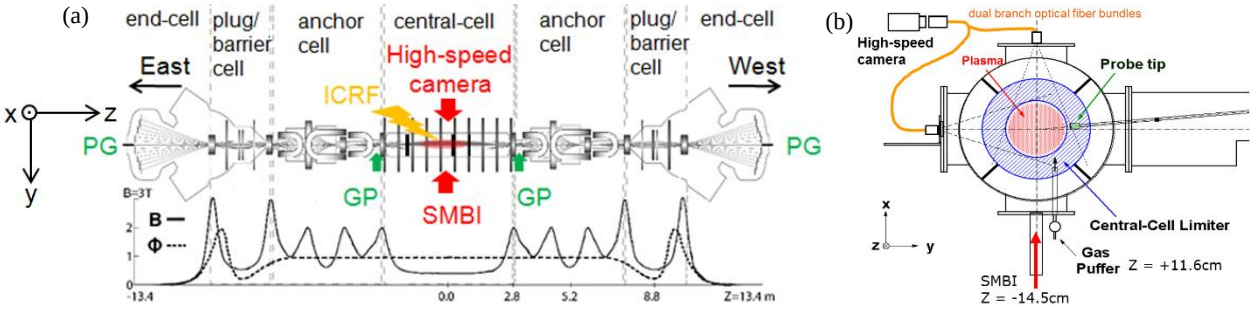

FIGURE 1 (a) Schematic view of GAMMA 10 and axial profile of magnetic field strength B and potential ϕ. (b) Cross-sectional view of the central-cell, location of SMBI system and high-speed camera.

EXPERIMENTAL RESULTS

In the experiment, SMBI pulse was injected into ICRF heated plasmas of GAMMA 10. The response of the gas fueling by SMBI with Laval nozzle to the electron density was investigated by changing the SMBI plenum pressure [11]. Figure 2(a) shows a typical of 2-D image of visible emission during SMBI from the GAMMA 10 plasma captured by fast camera. These 2-D images are captured at the timing of the peak emission intensity. The peak emission occurs at 1.2 ms after the SMBI. It implies that SMBI with Laval nozzle is faster than that of straight nozzle [6]. The left side of Fig. 2(a) shows the emission intensity emitted in the vertical direction and the right side shows intensity emitted in the horizontal direction. In order to investigate the directivity of the injected molecular beam by SMBI, axial profile of neutral transport was investigated based on the 2-D image from vertical direction. The full width at half maximum (FWHM) of the emission intensity at $y = 0$ is calculated as an index of the axial neutral transport. Since the shape of the intensity profile i.e. FWHM is not sensitive to its intensity strength, FWHM at the timing of the peak intensity is used. We analyzed the FWHM for each plenum pressure. Figure 2(b) shows the relationship between FWHM and plenum pressure of SMBI with Laval nozzle. The FWHM value with Laval nozzle is lower than that for the both cases with straight nozzle and without nozzle [5, 6]. Besides, in all plenum pressure, the FWHM value is lower than the plasma diameter. This means that the Laval nozzle has capability to improve the directivity of the particle fueling by SMBI. The FWHM value decreases with increasing the plenum pressure under the lower pressure (≤ 1 MPa) condition, while it saturates above 1 MPa. This means that the directivity of the particle was suppressed by the collision between neutral particles in the case of higher plenum pressure.

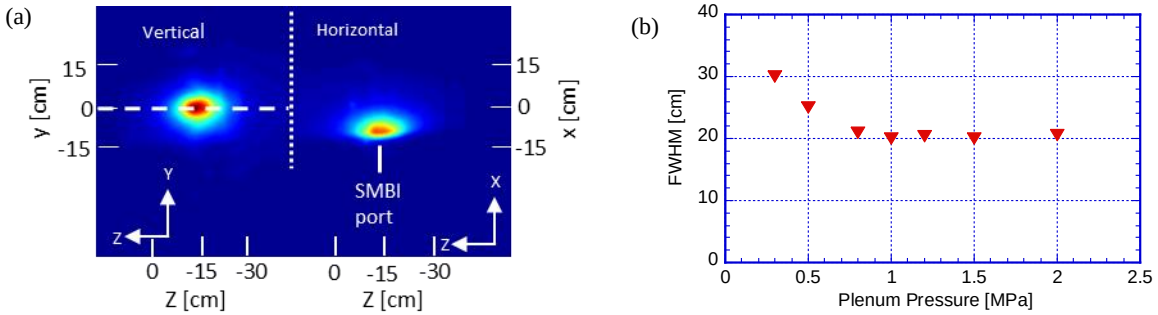

FIGURE 2 (a) 2-D image of the plasma during SMBI, (b) FWHM of emission intensity versus plenum pressure.

SIMULATION METHOD

Monte-Carlo simulation code (DEGAS) was performed in order to analyze the behavior of neutral particle in GAMMA 10. Three-dimensional mesh-model for DEGAS has been applied to the central-cell [12]. The limiters and antennae of the ICRF are precisely implemented in a realistic configuration in this model. Furthermore, this mesh model was improved for modeling SMBI experiments; it was expanded around the SMBI injection port and new mesh was added in a realistic configuration concerning the SMBI valve with Laval nozzle. A schematic of the vicinity of the Laval nozzle was also shown in Fig. 3(a). The background plasma parameters ($T_e \approx 40$ eV, $T_i \approx 5$ keV, $n_e = n_i \approx 2.0 \times 10^{12}$ cm^{-3}, etc) on each mesh was given based on the experimental data. The axial distribution of Hα emission was evaluated to investigate the neutral transport during SMBI. We introduce σ_{div} to index the divergence angle of the initial particles to simulate the molecular beam injected by SMBI. If the angular profile of launched particles has a cosine distribution, the divergence-angle index is $\sigma_{div} = 1.0$, if $\sigma_{div} = 0.5$, for example, the horizontal component of the velocity vector in the cosine distribution is reduced to half as shown in Figs. 3(b) and 3(c).

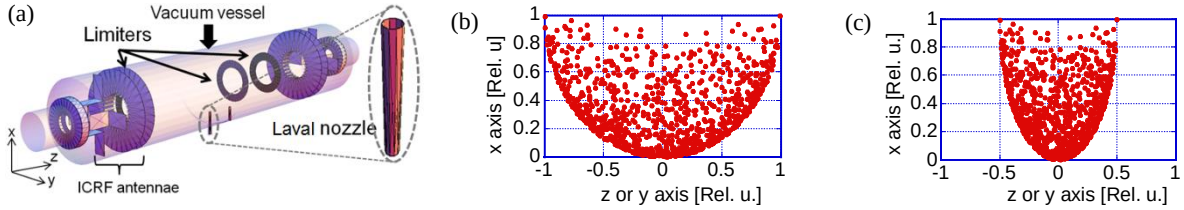

FIGURE 3 (a) Fully 3-dimensional DEGAS mesh model including SMBI with Laval nozzle, (b) Schematic view of distribution of launched particles, $\sigma_{div} = 1.0$ (cosine distribution), (c) $\sigma_{div} = 0.5$.

SIMULATION RESULTS

The axial distribution of the Hα emission near the SMBI injection port is calculated by DEGAS to investigate the behavior of neutral particle from SMBI. The 2-D Hα image calculated by DEGAS are shown in Figs. 4 (a)-(d), have the consistency with captured by the high-speed camera in Fig. 2(a). The 2-D Hα image was calculated by DEGAS for five different conditions; $\sigma_{div} = 1.0, 0.75, 0.5, 0.33\ and\ 0.25$. As shown in Figs. 4 (a)-(d) we observed that the dispersion of particles can be reduced by decreasing the divergence angle index and the emission area become more convergent. It has been also observed that the plenum pressure correlate with divergence angle index. Figure 4(e) shows the variation of Hα emission intensity with divergence angle index for five cases of divergence-angle index. The Hα emission intensity peak becomes narrower by decreasing the divergence angle index that we observed in Hα 2-D image. In the simulation, we evaluate the FWHM of the distribution of Hα as an index of the axial neutral transport in the same way as the experimental results. The comparison between experimental and simulation results are shown in Fig. 4(f). The hatched zone in shows the FWHM obtained from the experimental results. The FWHM value calculated by DEGAS depends on the divergence angle index and were the value close to the experimental results in the initial conditions of $\sigma_{div} = 0.5$ and $\sigma_{div} = 0.33$. However the simulation results could not reproduce the saturation of FWHM value in the experimental results. The reason would be that the DEGAS code takes no account of the collision between neutral particles. The SMBI with Laval nozzle must be modeled under the initial particle condition of $\sigma_{div} = 0.33\ to\ 0.5$ to reproduce the experimental results for a plenum pressure between 0.3 to 2.0 MPa.

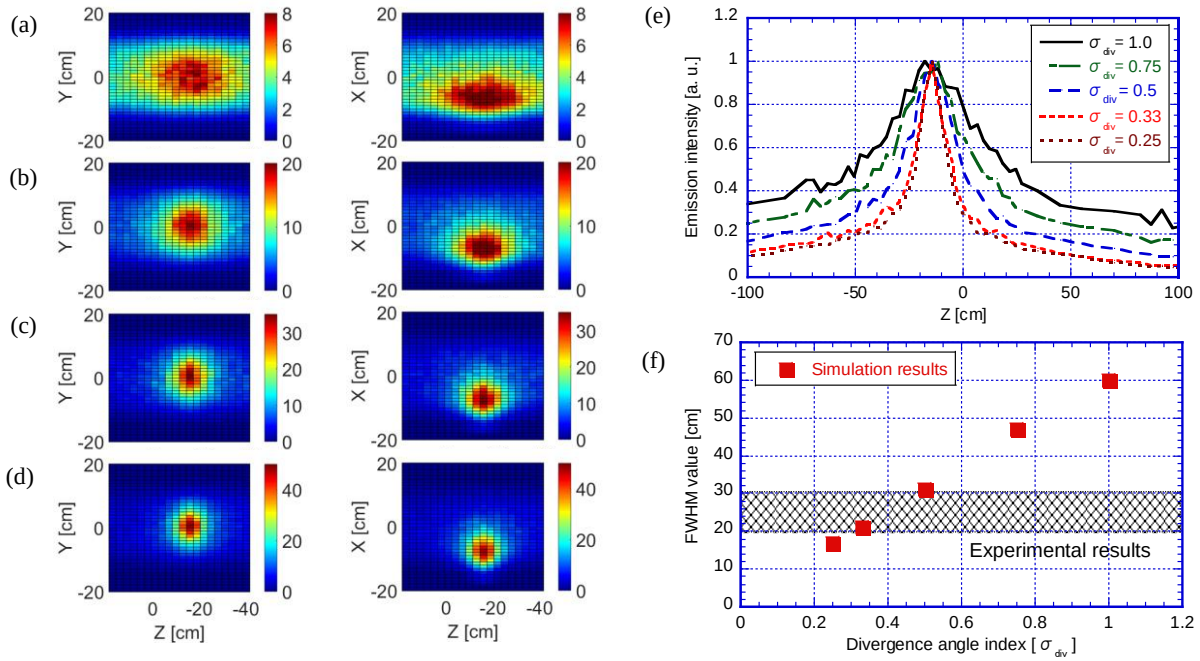

FIGURE 4 (a) 2-D Hα image calculated by DEGAS code (a) $\sigma_{div} = 1.0$, (b) $\sigma_{div} = 0.5$, (c) $\sigma_{div} = 0.33$, (d) $\sigma_{div} = 0.25$, (e) axial distribution of the emission calculated by DEGAS, (f) FWHM of emission intensity versus divergence angle index.

SUMMARY

Neutral particle transport during SMBI with Laval nozzle was investigated in both experiments and simulations. According to the experimental results obtained by the high-speed camera, the diffusion of neutral particle could be suppressed more by Laval nozzle than the straight nozzle. However FWHM value was saturated in the higher plenum pressure. The simulation results qualitatively reproduced the experimental results. This results will enable us to discuss the spatial structure for investigating the penetration depth. Above results contribute to the optimization of fueling. In future works, radial profile of neutral transport in GAMMA 10 will be investigated in detail for optimization of fueling by SMBI with Laval nozzle.

ACKNOWLEDGMENTS

This study was supported by the bilateral collaboration research program in the University of Tsukuba, Kyoto University, and Hiroshima University (NIFS12KUGM068, NIFS12KUHL050 and NIFS12KUGM065). The author thanks the members of the GAMMA 10 group for their collaboration on the experiments and for helpful discussion.

REFERENCES

[1] L. Yao et al., Nucl. Fusion **47**, 1399 (2007).
[2] D. L. Yu et al., Nucl. Fusion **50**, 035009 (2010).
[3] D. L. Yu et al.,Nucl. Fusion **52**, 082001 (2012).
[4] M. Inutake et al., Phys. Rev. Lett. **55**, 939 (1985).
[5] K. Hosoi et al., Plasma Fusion Res. **9**, 3402087 (2012).
[6] K. Hosoi et al., Fusion Sci. Technol. **63**, 244 (2013).
[7] D. Heifetz, D. Post, M. Petravic et al., J. Comput. Phys. **46**, 309 (1982).
[8] Y. Nakashima et al., J. Nucl. Mater. **196-198**, 493 (1992).
[9] Y. Nakashima et al., J. Nucl. Mater. **313-316**, 553 (2003).
[10] T. Cho, H. Higaki et al., Fusion Sci. Technol. **47** No.1T 9-16 (2005).
[11] M.M. Islam et al., Plasma Fusion Res. **11**, 2402053 (2016).
[12] Y. Nakashima et al., J. Plasma Fusion Res. SERIES **6**, 546 (2004).